ELEVATOR GROUP CONTROL AS A CONSTRAINED MULTIOBJECTIVE OPTIMIZATION PROBLEM

A PREPRINT

Aljoša Vodopija
Jožef Stefan International Postgraduate School
Ljubljana, Slovenia
aljosa.vodopija@ijs.si

Bogdan Filipič
Department of Intelligent Systems,
Jožef Stefan Institute,
Ljubljana, Slovenia

Jörg Stork
IDE+A, TH Köln
Steinmüllerallee 1
51643 Gummersbach
joerg.stork@th-koeln.de

Thomas Bartz-Beielstein
IDE+A, TH Köln
Steinmüllerallee 1
51643 Gummersbach
thomas.bartz-beielstein@th-koeln.de

ABSTRACT

Modern elevator systems are controlled by the elevator group controllers that assign moving and stopping policies to the elevator cars. Designing an adequate elevator group control (EGC) policy is challenging for a number of reasons, one of them being conflicting optimization objectives. We address this task by formulating a corresponding constrained multiobjective optimization problem, and, in contrast to most studies in this domain, approach it using true multiobjective optimization methods capable of finding approximations for Pareto-optimal solutions. Specifically, we apply three multiobjective evolutionary algorithms with default constraint handling techniques and demonstrate their performance in optimizing EGC for nine elevator systems of various complexity. The experimental results confirm the scalability of the proposed methodology and suggest that NSGA-II equipped with the constrained-domination principle is the best performing algorithm on the test EGC systems. The proposed problem formulation and methodology allow for better understanding of the EGC design problem and provide insightful information to the stakeholders involved in deciding on elevator system configurations and control policies.

1 Introduction

Elevator systems gave architects new degrees of freedom and allowed buildings to become as multifaceted as they are today. The well-functioning of these transport systems is often taken for granted in our modern, barrier-free life in urban areas. To realize this, most modern elevator systems are controlled by so-called elevator group controllers, which optimize the respective systems' service quality. Based on the passenger's desired destination, they assign moving and stopping policies to the elevator cars. Creating an adequate elevator group control (EGC) policy depicts a complex problem, which involves multiple objectives and further depends on the elevator systems and building structure variables. The objectives include, besides passenger satisfaction, energy consumption, and material attrition. The resulting multiobjective optimization function is highly nonlinear and multimodal, highly dynamic, and stochastic, mainly because passengers do not arrive in a deterministic manner, but based on a stochastic process. These problem properties render classic, gradient-based optimizers as not applicable and require advanced search strategies [1].

The presence of multiple conflicting objectives is a particularly notable characteristic of EGC. However, while EGC design is often referred to as a multiobjective optimization problem, it was approached with true multiobjective optimizers—in the sense of finding trade-offs between the objectives—only in our preliminary study in this domain [2]. In that study, we proposed a bi-objective problem formulation of the EGC optimization problem and used the sequential ring (S-Ring) model [3] to evaluate the solutions of the resulting optimization problem. In more detail, we dealt

with two objectives that are often studied in the literature, and both need to be minimized: the average number of states with waiting passengers and the total number of elevator stops [4, 5, 6]. While the first objective is directly associated with passenger satisfaction, the second objective reflects both energy consumption and material attrition. It is worth noting that the two objectives are conflicting in nature since a prompt EGC service that would reduce the number of states with waiting passengers requires many elevator car stops. A true multiobjective optimization approach is needed to obtain a set of trade-off solutions if preferences between the objectives are not known in advance. For this purpose, we applied multiobjective evolutionary algorithms (MOEAs) to find the fronts of trade-off solutions. The approach was tested on three real-world elevator systems, confirmed the methodology's suitability, and offered relevant insights into problem properties.

However, a deeper analysis of the results obtained in [2] revealed that many produced solutions allow for a large number of elevator car skips. For example, in test problems reflecting residential buildings, passengers faced more than 20 elevator car skips, making such EGC policies inadmissible for practical use.

In this paper, we address the related issue by extending the initial bi-objective formulation with a constraint that limits the number of elevator car skips. The addition of this constraint fundamentally changes the EGC optimization problem and requires dedicated algorithms to solve the resulting constrained multiobjective optimization problem. In contrast to the related work, we do not combine the objectives into a single function (the weighted-sum approach) but use true constrained multiobjective optimization. In particular, we deployed three widely used MOEAs featuring the constrained-domination principle and the penalty function approach. The MOEAs are systematically tuned to provide as unbiased results as possible. A new set of nine test elevator system configurations, ranging from simple to very complex ones, is composed to study the problem's hardness and test the applied algorithms' scalability. The results are thoroughly analyzed from the aspects of the solution quality and the algorithm performance, and specific problem characteristics. Finally, the superiority of using true multiobjective optimization over the weighted-sum approach is also demonstrated.

The paper is further organized as follows. Section 2 reviews the related work in EGC, focusing on various aspects of the problem. Section 3 presents the S-Ring model used to simulate EGC and perform its optimization. Section 4 formulates EGC as a constrained multiobjective optimization problem. Section 5 reports on the conducted numerical experiments and analyzes their results. Section 6 concludes the paper by summarizing the work done and the essential findings and providing future work ideas.

2 Related Work

In this section, we provide a detailed review of the related work. We first address relevant aspects of dealing with EGC design including general control issues, changing environments, and passenger traffic forecast. Next, special attention is devoted to the optimization of EGC systems. In particular, simulation models as a prerequisite for optimization are described. Optimization in the presence of multiple objectives is also discussed. Finally, we conclude by presenting new elevator concepts and strategies.

2.1 Efficient Control

Efficiency is a demanding issue in EGC. Computationally cheap methods become more and more important, especially in high-rise buildings with many passers-by. Banks of elevators are working in parallel in these buildings. They are required to serve the populace efficiently and quickly. For this purpose, Mahmut et al. [7] designed a control mechanism such that each call will be served by the elevator deemed to be the most energy-efficient. The control mechanism used was derived from the ground up using simple calculations to be computationally cheap, fast, and implementable with the most basic microcontroller. In Sahin et al. [5], a real-time monitoring system is installed to reduce redundant stops, and improve passenger comfort and energy consumption.

Because high-rise buildings require many elevators, they can be optimized group-wise. Utgoff and Connell [8] proposed an algorithm for dispatching cars to maximize efficiency for all the individuals who use an elevator in the group of elevators. Much information about the individuals in the group is inferred or estimated, greatly aiding the decision-making process. Insights are offered into the nature of various objective functions and their effects on system performance.

2.2 Changing Environments

EGC strategies, which consider demand changes over time and different traffic patterns and differences between floors (or zones), are subject to on-going research. Fujino et al. [9] presented a concept for EGC systems that can

change control settings according to individual floor utilization situations. The floor-attribute-based control method uses a combination of floor-attribute-based evaluation and car-attribute-based evaluation. The authors propose an online parameter tuning method using genetic algorithms. Pepyne and Cassandras [10] developed optimal dispatching controllers for elevator systems during peak traffic. A peak traffic period arises during the start of a business day in office buildings where many passengers are moving from the first floor up into the building. The cars deliver the passengers and then return empty to the first floor to pick up more passengers. The authors propose a threshold-based policy that dispatches an available car from the first floor when the number of passengers inside the car reaches or exceeds a threshold that depends on several factors, including the passenger arrival rate, elevator performance capabilities, and the number of elevators available at the first floor. Because most elevator systems have sensors to determine the car locations and the number of passengers in each car, such demand-driven policies can be easily implemented in EGC systems. Dynamic programming techniques are standard tools for obtaining optimal control policies.

2.3 Prediction

Robust dispatching decisions require that future passenger traffic is forecast based on the realized passenger flow in a building. EGC optimization can be combined with prediction methods. Thus, EGC dispatches elevators to passengers' calls in a dynamic environment where new calls continuously emerge. When making a dispatching decision, it is not known when and at which floors new passengers will register new calls, what is the number of passengers waiting behind these and existing calls, and what are their destinations. The problem is that this flow cannot be directly measured. However, it can be estimated by finding the passenger counts for the origins and destinations of every elevator trip occurring in a building. An elevator trip consists of successive stops in one direction of travel with passengers inside the elevator. Kuusinen et al. [11] formulated the elevator trip origin-destination matrix estimation problem as a minimum cost network flow problem and developed a branch-and-bound algorithm.

2.4 Simulation-based optimization

Optimization of real elevator systems is an important technique. In addition to elevator test stands (elevator towers), simulators are valuable tools in EGC optimization. For example, the multi-car elevator (MCE) simulator is a popular open-source implementation [12].

However, it is also of great interest to use a simulator, which implements the essential features of an EGC system only and does not require the specification of too many details. Results from this essential simulator can be easily compared between various elevator implementations. This idea inspired Markon et al. [13, 14] to develop the S-Ring (sequential ring). The S-Ring is a simplified model of a complex discrete dynamic system, i.e., an EGC system. The proposed model, which is a simplified model of elevator group control, has most of the properties that make the elevator group control problem challenging and popular, but in contrast to elevator models, it is simple and easily reproducible. It can be used as a benchmark for EGC optimization studies. The optimal control problem of the S-Ring can be formulated as a dynamic programming problem [15]. The S-Ring system is constructed in a way that balances between two conflicting requirements: it retains the most critical dynamical characteristics of the EGC system, but at the same time, it allows for exact solutions by algorithmic methods. As a concrete example, Markon [3] derived the S-Ring model from a formal model of EGC, described the solution process, and illustrated using the exact solution to benchmark some optimization methods. He also described a variant, the S-Lane model, and showed its solution as an example of extending the technique to related problems.

In [1], Bartz-Beielstein et al. used the S-Ring to benchmark single-objective heuristics. Using the S-Ring model, it is possible to retain a high level of complexity and optimize an EGC control strategy using modern heuristics with a high number of strategy evaluations while keeping a feasible computational load.

Onat et al. [16] used the S-Ring for comparing different reinforcement learning schemes and stochastic approximation and Q-learning. Bartz-Beielstein et al. [14] demonstrated that a Nelder-Mead simplex algorithm and a quasi-Newton method could not escape from local optima while optimizing the S-Ring. In contrast to the artificial test functions from commonly used test-suites, real-world optimization problems often have many local optima on flat plateaus. The distribution of local optima in the search space of the S-Ring is unstructured. Therefore, these algorithms were unable to escape plateaus of equal function values. The analysis of S-Ring optimization reveals that evolution strategies are flexible optimization tools.

2.5 Multiobjective optimization

Ruokokoski et al. [17] studied the EGC problem arising in destination controls, because in many standard EGC optimization methods, a routing aspect is not considered: decision variables specify only request-to-elevator assignments.

The average waiting time and average journey time are used as objective functions in the comparisons. This example shows that the ECG optimization problem can be formulated in the context of multiobjective optimization. Finding a suitable control strategy for the EGC is a complex optimization problem with several objectives.

Surprisingly, despite EGC optimization problems are widely discussed and known for involving conflicting objectives, they are seldom solved with multiobjective optimization. For example, Hakonen et al. [4] utilized a set of objectives, such as the passenger waiting time, the ride time, and the total number of elevator stops but combined them linearly into a single objective. Tyni and Ylinen [6] used a weighted aggregation method to optimize the landing call waiting time and energy consumption with an evolutionary algorithm in a real-time environment.

In contrast, in [2], we for the first time addressed the EGC optimization problem with a true multiobjective optimization approach. In particular, we used the S-Ring model to evaluate the solutions for the bi-objective problem formulation and applied MOEAs to find the fronts of trade-off solutions.

2.6 New Elevator Concepts

Takahashi et al. [18] analyzed multi-car elevator systems, which are revolutionary new technology for high-rise buildings [19, 20, 21]. In such a vertical transportation application using a rope-less elevator, the design of linear motors with a high ratio of payload to self-weight becomes an impotent issue. The basic requirement for a linear motor for the rope-less elevator system is smooth motion, high driving force, and lightweight. Takahashi et al. [18] investigated the optimal design of such motors for multi-car linear motor elevator applications. Onat et al. [22] and Gurbuz et al. [23] performed a multiobjective optimization of these new motors using evolution strategies.

3 S-Ring Model

The S-Ring is a discrete, nontrivial event system to simulate elevator group control [3]. It is highly adaptable and thus applicable to different use-cases while maintaining low implementation effort. The system's primary focus is to model the operation of an elevator system by simulating the handling of passenger traffic and passenger serving. It is intended to serve as a dynamic, fast to evaluate, and computationally inexpensive system for optimization purposes, i.e., finding solutions for EGC systems that serve passengers in the fastest, most energy-efficient, and most comfortable way. Due to its low computational costs, the S-Ring can quickly evaluate a broad variety of EGC systems as benchmarks for the proposed multiobjective optimization approach. In general, the S-Ring consists of three key elements: state-space representation, state transition table, and control policy.

3.1 State-Space Representation

To simulate an EGC system, the S-Ring utilizes states for passengers, c_i, as well as elevator cars, e_i, $i = \{1, \ldots, N_s\}$. The size of the state space, i.e., the number of states in the system, is determined by the number of floors, n. Each floor has a double set $s_i = \{c_i, e_i\}$ of a passenger, and elevator car states for the upward and downward direction. An exception are the lowest and top floor, with only a single set of states. This results in a total number of $N_s = 2n - 2$ states for a system. An example of an EGC system with the related S-Ring model is illustrated in Figure 1. During the simulation, the maximum number of possible active elevator states is equal to the number of available elevator cars, m. Moreover, the number of active passenger states is dynamically changing over time and is influenced by the probability of a new arriving passenger, p.

3.2 State Transition Table

The fixed and dynamic rules for state transition in the current position of the S-Ring are displayed by the state transitions (Table 1), which is applicable for each state set in the S-Ring simulator [24]. For illustration, the current state sets s_i are extended by the subsequent elevator state, forming state triplets c_i, e_i, e_{i+1}, e.g., 101 for a waiting passenger (1xx), no elevator car on the current floor (x0x) and a car on the next floor (xx1). Moreover, the state transitions are influenced by the probability of arrival (p) or no arrival ($1 - p$) of a new passenger. Some states do not require or allow a policy decision and lead to predetermined transitions. At each state, it is first checked whether a new passenger arrived. Next, if the current state is an active elevator state, the controller determines whether the elevator car stops or continues to the next state. Finally, the indication of the passenger active state is updated depending on whether or not the passengers were served.

Table 1: State transition table for the S-Ring. The table shows the states and decisions to be made in certain states. The transition probabilities are influenced by the probability of arrival (p) or no arrival ($1-p$) of a new passenger and the control policy. The states are encoded in the following way: $1**$ indicates a passenger present, $*1*$ an elevator present, and $**1$ a passenger waiting on the next floor. If $p = 1$, a new passenger arrives. Some states have fixed transitions and do not require a policy decision.

Current state s_i	Transition probability	Policy π	Next state s_{i+1}	Δc_i
000	$1-p$		000	0
	p		100	-1
100	1		100	0
010	$1-p$		001	0
	p	0	101	-1
		1	010	0
110	1	0	101	0
		1	010	$+1$
001	$1-p$		001	0
	p		101	-1
101	1		101	0
011	1		011	0
111	1		011	$+1$

3.3 Control Policy

The control policy π establishes the decision of either serving or passing a passenger for the required state transitions and is the key objective for any optimization. In general, an optimized policy could be realized by a lookup table if n remains very small. However, for large n this becomes infeasible, and a neural network (NN) perceptron is utilized to perform the state-to-decision mapping [24]. The NN uses a simple, direct structure without hidden layers. The inputs, i.e., the states of the S-Ring, are directly connected to a binary output with an adjacent weight vector of length $2N_s$. For a given setup of n, m, and p, the perceptron's size remains fixed, and the state to decision mapping is only influenced by the weight vector $\vec{w}$ of the NN controller, which is also the main target of any optimization.

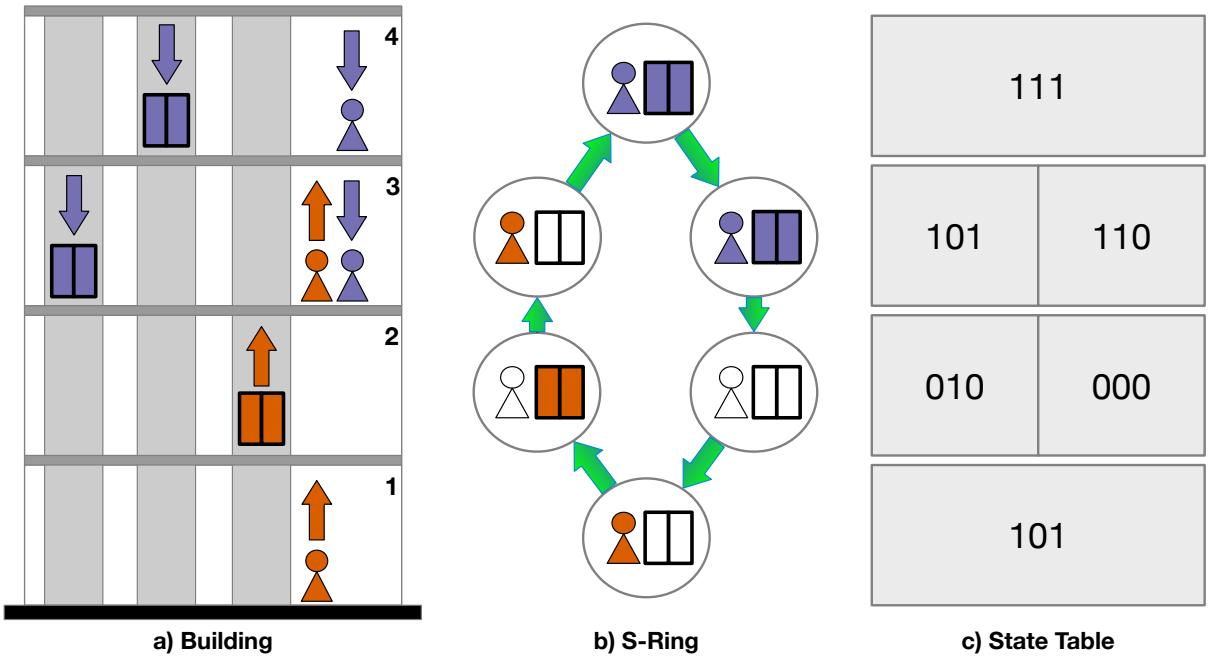

Figure 1: S-Ring model with related building and state table. a) shows a building with three elevator cars, four floors, and two waiting passengers for each direction. Upwards and downwards direction is possible for elevators and passengers and are colored red and blue, respectively. b) illustrates the S-Ring model for this building, with a single state for the top and ground-floor and two states for the rest. c) displays the state encoding for each of the S-Ring states.

4 Problem Formulation

In this section, we propose a multiobjective formulation of the EGC optimization problem. Specifically, we deal with two EGC objectives that are often studied in the literature, and both need to be minimized: the average number of states with waiting passengers, and the total number of elevator stops [4, 5, 6]. In contrast to previous publications, we do not combine the objectives into a single function but adopt the multiobjective perspective. Moreover, to make it possible to compare the performance of elevator systems of various configurations (determined by the number of floors n and the number of elevator cars m), we consider normalized objective function values.

The first objective (h_1) is the proportion of states with waiting passengers. It is expressed as the average number of states with waiting passengers, M_w, divided by the number of all states, N_s:

$$h_1 = \frac{M_w}{N_s}. \tag{1}$$

The second objective (h_2) is the proportion of elevator stops. It is equal to the total number of elevator stops, M_t, divided by the maximum possible number of elevator stops. The latter can be calculated as the number of elevator cars m multiplied by the number of EGC simulation cycles, which in turn corresponds to the number of state transition steps, N_t, divided by the number of states, N_s, therefore

$$h_2 = \frac{M_t}{mN_t/N_s}. \tag{2}$$

Intuitively, the passengers' discomfort with long waiting times and long riding times due to many elevator stops does not increase linearly with time, but more drastically. To model this effect, we have additionally modified the original objectives as

$$f_1 = h_1^{\alpha} \quad \text{and} \quad f_2 = h_2^{\beta}, \tag{3}$$

where $\alpha, \beta \in [1, 2]$ are the objective function coefficients. The choice of their values is subjective, but the idea is to reflect the elevator system characteristics and the passenger preferences.

In our previous work on EGC [2], we observed that many obtained solutions allow for a large number of elevator car skips. It sometimes happened that a passenger was skipped more than 20 times, which made an EGC policy impractical. In this work we therefore introduce a constraint that renders all solutions with a large number of elevator skips infeasible. The corresponding constraint is expressed as the maximum number of elevator skips, M_s, that has to be less than or equal to M, therefore:

$$c = M_s \leq M. \tag{4}$$

The resulting constrained multiobjective optimization problem (CMOP) can be mathematically formulated as

$$\begin{aligned} &\text{minimize} \quad f_m(\vec{w}), \quad m = 1, 2 \\ &\text{subject to} \quad c(\vec{w}) \leq M \end{aligned} \tag{5}$$

where $\vec{w} = (w_1, \ldots, w_D)^{\mathrm{T}}$ is a perceptron weight, $f_1, f_2 : [-1, 1]^D \to \mathbb{R}$ are the two objective functions, $c : [-1, 1]^D \to \mathbb{R}$ is the constraint function, and $[-1, 1]^D$ the decision space of dimension $D = 2N_s$. Additionally, $f_m(\vec{w})$ is an objective value and $\phi(\vec{w}) = \max(c(\vec{w}) - M, 0)$ constraint violation.

5 Experiments and Results

This section first introduces test elevator system configurations used in the experimental analysis of the considered EGC optimization problem. Then, we present multiobjective evolutionary algorithms (MOEAs), constraint-handling techniques (CHTs), and the parameter tuning used in this study. Finally, we analyze the performance of the applied MOEAs as well as investigate the complexity of the introduced test configurations.

5.1 Test Elevator System Configurations

Table 2 summarizes the test elevator system configurations used to assess the performance of multiobjective optimization approaches in our experiments. Nine configurations were carefully selected to cover a wide range of elevator systems operating in various kinds of buildings. The number of floors determines the building size. It varies among 5, 20, and 50. The probability of newly arriving passengers takes values among 0.01, 0.05, and 0.1. The smallest probability reflects elevator systems operating in environments with low passenger traffic, such as residential buildings. On

the other hand, the probability of 0.1 is connected to very high passenger traffic observed in commercial buildings or parking garages. The number of elevator cars was selected based on building size and passenger traffic. The idea was to reflect real and meaningful elevator systems. Finally, the parameters α, β were set to 1.5 and M to 4 for all test configurations.

Table 2: Characteristics of the test elevator system configurations: number of floors n, number of elevator cars m, probability of new arriving passenger p, number of states in the S-Ring representation N_s.

Config.	n	m	p	N_s
C1	5	1	0.01	8
C2	5	2	0.05	8
C3	5	3	0.10	8
C4	20	4	0.01	38
C5	20	6	0.05	38
C6	20	8	0.10	38
C7	50	10	0.01	98
C8	50	15	0.05	98
C9	50	20	0.10	98

5.2 Experimental Setup

Based on the constrained multiobjective formulation of the EGC optimization problem, the experimental evaluation aimed at finding sets of trade-off feasible solutions representing approximations for Pareto fronts. For this purpose we used three well-known MOEAs equipped with their default CHTs: Nondominated Sorting Genetic Algorithm II (NSGA-II) [25], Differential Evolution for Multiobjective Optimization (DEMO) [26], and Multiobjective Evolutionary Algorithm based on Decomposition (MOEA/D) [27]. In addition, random search (RS) was run as a baseline optimizer to verify that our experimental setup was well designed.

The constrained domination principle (CDP) [25] was used in NSGA-II and DEMO. This approach extends the dominance relation and is one of the most widely-used techniques for constrained multiobjective optimization. CDP strictly favors feasible solutions over infeasible ones. It ranks feasible solutions based on Pareto dominance and infeasible solutions based on constraint violation values. The formal definition of CDP, as introduced in [25], is provided with the following rule.

A solution $\vec{w}$ is said to constrained-dominate a solution $\vec{v}$, if any of the following conditions is true.

1. Solution $\vec{w}$ is feasible and solution $\vec{v}$ is not ($\phi(\vec{w}) = 0$ and $\phi(\vec{v}) > 0$).
2. Solutions $\vec{w}$ and $\vec{v}$ are both infeasible, but solution $\vec{w}$ has a smaller overall constraint violation ($\phi(\vec{w}) < \phi(\vec{v})$).
3. Solutions $\vec{w}$ and $\vec{v}$ are feasible and solution $\vec{w}$ dominates solution $\vec{v}$ ($\phi(\vec{w}) = \phi(\vec{v}) = 0$ and $\vec{w} \preceq \vec{v}$).

CDP can be integrated into NSGA-II and DEMO in the replacement phase, i.e., survivor selection, where dominance relation is replaced with CDP. The rest of NSGA-II and DEMO is kept unchanged.

On the other hand, an approach based on the penalty function was considered in MOEA/D [28]. In MOEA/D, the aggregation function (Tchebycheff function in our study) is enhanced with a penalty term according to the following formula:

$$f^p(\vec{w} \mid \gamma) = f^{te}(\vec{w} \mid \lambda, z^\star) + \gamma\phi(\vec{w}). \tag{6}$$

Here, f^{te} is the Tchebycheff aggregation function, $\gamma > 0$ the penalty weight, and ϕ constraint violation. This enhanced aggregation function is used to compare solutions in the update phase of MOEA/D.

Evolutionary methods involve various parameters controlling their operation. The choice of parameter values can profoundly impact the algorithm performance. Thus, in many real-world applications, it is mandatory to select an adequate set of algorithm parameter values to solve the given problem efficiently. Besides, the adequate choice of parameter values allows for a more sound and robust comparison of various algorithms. This is because an algorithm's chance to be inferior due to an inappropriate choice of parameter values is highly reduced.

In the literature, various approaches to tuning or controlling algorithm parameters have been proposed. However, one of the most reliable and efficient methods used for real-world problems remains sequential model-based parameter optimization. This approach falls in the group of parameter tuning methods and is one of the most frequently used approaches when dealing with computationally demanding evaluations. In this paper, Sequential Parameter Optimization (SPO) [29] was used to tune the algorithm parameters.

The target function optimized by SPO was the MOEA performance measured as the obtained cumulative hypervolume given the algorithm parameter settings. The target function's decision variables were the following algorithm parameters: the population size, n_p, ranging from 48 to 500, the crossover probability, p_c, and the mutation probability, p_m, both taking values from $[0, 1]$. The scaling factor, F, was tuned instead of the mutation probability in DEMO. The number of generations, n_g, was computed as the number of solution evaluations, f_e, divided by the population size:

$$n_g = \left\lceil \frac{f_e}{n_p} \right\rceil . \tag{7}$$

Therefore, it was not considered as a decision variable (algorithm parameter) by the tuning process. The number of allowed solution evaluations changed proportionately with the number of floors: $f_e = 2000n$. Note that $n_g n_e$ may be greater than f_e. If this happened, the run was prematurely stopped after f_e solution evaluations.

Additionally, we used the following SPO configuration: Gaussian process regression for building surrogate models, classic differential evolution as the optimizer, Latin hypercube sampling (LHS) to initiate the algorithm parameters, and 25 target function evaluations (MOEA runs) without repetitions. The tuned algorithm parameter values aggregated over configurations of the same size are summarized in Table 3.

Table 3: Tuned algorithm parameter values aggregated over test elevator system configurations of the same size: total number of solution evaluations f_e, population size n_p, number of generations n_g, crossover probability p_c, mutation probability p_m, and scaling factor F.

Config.	f_e	NSGA-II				DEMO				MOEA/D			
		n_p	n_g	p_c	p_m	n_p	n_g	p_c	F	n_p	n_g	p_c	p_m
C1, C2, C3	10,000	120	84	0.78	0.46	328	31	0.29	0.22	204	50	0.77	0.50
C4, C5, C6	40,000	240	167	0.79	0.16	264	152	0.55	0.34	120	334	0.59	0.32
C7, C8, C9	100,000	180	556	0.91	0.17	432	232	0.58	0.42	408	246	0.70	0.11

5.3 Implementation

All the algorithms and functionalities needed for this study are implemented in the R programming language [30]. The experiments with NSGA-II and MOEA/D were carried out using the R packages `mco` and `MOEADr`, respectively. On the other hand, the DEMO algorithm was re-implemented in R from scratch and is available at [31]. Finally, SPO, as implemented in the `SPOT` R package, was used in the tuning phase.

An R package including the code used in this study and an R vignette explaining all the functionalities can be found in the GitHub repository [31]. The package allows for further experimentation with additional elevator configurations and can be freely used under the conditions determined by the GNU General Public License, version 3 [32].

5.4 Results

The algorithms were assessed from the point of view of both effectiveness (quality of results) and efficiency (required execution time). To assess the algorithm effectiveness, every algorithm was run 31 times, each time with a new randomly initialized population of solutions and the tuned parameters from Table 3. The cumulative hypervolume of the Pareto front approximation and the cumulative inverted generational distance plus (IGD^+) were used to measure the quality of results. Cumulative means that all the nondominated feasible solutions found in the entire run were used for hypervolume and IGD^+ calculation. Given $f_1, f_2 \in [0, 1]$, the reference point for hypervolume calculation was set to $(1.1, 1.1)^{\mathrm{T}}$. Additionally, all the nondominated feasible solutions found over all runs and algorithms were used as a reference front for calculating IGD^+.

The means of cumulative hypervolume and IGD^+ values averaged over 31 runs are shown in Table 4 and Table 5, respectively. The results indicate that RS performs comparably to MOEAs on C1 and C2 according to the obtained hypervolume values, and it underperforms on other test configurations. According to IGD^+, RS is always outperformed by MOEAs.

As we can see, for all three MOEAs, the obtained hypervolume and IGD^+ values are very similar on C1–C4. In contrast, NSGA-II performs noticeably better than DEMO and MOEA/D on C5–C9 concerning IGD^+. Besides, NSGA-II outperforms both algorithms on C5, C6, C8 and C9 with respect to hypervolume, while on C7 only MOEA/D is outperformed by NSGA-II. Finally, only negligible differences are observed between DEMO and MOEA/D performance on C5, C6, C8 and C9 with respect to hypervolume and IGD^+.

The statistical analysis confirms these findings. According to Friedman test, we observe statistically significant differences in MOEA performance concerning both hypervolume ($\chi^2(2) = 13.556$, $p = 0.0011$) and IGD^+

Table 4: Average cumulative hypervolume values for all MOEAs on the test elevator system configurations.

Config.	NSGA-II	DEMO	MOEA/D	RS
C1	1.19 ± 0.00	1.19 ± 0.00	1.19 ± 0.00	1.19 ± 0.00
C2	1.10 ± 0.00	1.10 ± 0.00	1.10 ± 0.00	1.10 ± 0.00
C3	1.05 ± 0.00	1.05 ± 0.00	1.05 ± 0.00	1.03 ± 0.00
C4	1.16 ± 0.00	1.16 ± 0.00	1.15 ± 0.01	1.09 ± 0.01
C5	0.95 ± 0.00	0.92 ± 0.01	0.92 ± 0.02	0.75 ± 0.02
C6	0.79 ± 0.00	0.76 ± 0.01	0.77 ± 0.01	0.62 ± 0.02
C7	1.03 ± 0.01	1.02 ± 0.02	0.98 ± 0.04	0.79 ± 0.05
C8	0.69 ± 0.02	0.61 ± 0.02	0.63 ± 0.02	0.50 ± 0.00
C9	0.63 ± 0.01	0.59 ± 0.02	0.60 ± 0.02	0.47 ± 0.01

Table 5: Average cumulative IGD^+ values for all MOEAs on the test elevator system configurations.

Config.	NSGA-II	DEMO	MOEA/D	RS
C1	0.0007 ± 0.0002	0.0007 ± 0.0003	0.0006 ± 0.0002	0.0011 ± 0.0004
C2	0.0022 ± 0.0006	0.0023 ± 0.0006	0.0021 ± 0.0005	0.0055 ± 0.0011
C3	0.0025 ± 0.0005	0.0031 ± 0.0008	0.0056 ± 0.0018	0.0120 ± 0.0014
C4	0.0059 ± 0.0026	0.0074 ± 0.0004	0.0088 ± 0.0040	0.0482 ± 0.0074
C5	0.0090 ± 0.0025	0.0183 ± 0.0049	0.0195 ± 0.0064	0.1297 ± 0.0108
C6	0.0094 ± 0.0025	0.0254 ± 0.0038	0.0180 ± 0.0059	0.1356 ± 0.0145
C7	0.0118 ± 0.0047	0.0211 ± 0.0163	0.0476 ± 0.0034	0.1778 ± 0.0411
C8	0.0221 ± 0.0110	0.0569 ± 0.0130	0.0635 ± 0.0085	0.1442 ± 0.0027
C9	0.0118 ± 0.0041	0.0271 ± 0.0072	0.0287 ± 0.0108	0.1190 ± 0.0068

($\chi^2(2) = 10.889$, $p = 0.0043$). Post hoc analysis with Wilcoxon signed-rank test and Holm's correction to adjust p-values shows that NSGA-II performance is superior to those of DEMO and MOEA/D. On the other hand, no statistically significant differences are observed between DEMO and MOEA/D performance. The adjusted p-values of pairwise comparisons are shown in Table 6.

The execution times are reported in Table 7. As we can see, the execution times of NSGA-II and DEMO are comparable, while MOEA/D is less efficient. Besides, RS is significantly faster than MOEAs. However, the most computationally expensive task is the S-Ring simulation, where many perceptron evaluations are required. In general, solutions found by RS require only a negligible number of perceptron evaluations and are thus much faster but at the same time of low quality. Nevertheless, the EGC optimization considered here is a design problem, therefore efficiency is not of key importance.

The results can also be analyzed by visualizing the obtained Pareto front approximations. Figure 2 shows Pareto front approximations for the test configurations resulting from typical runs of MOEAs. In more detail, all the runs corresponding to a given test elevator configuration are sorted based on the obtained cumulative hypervolume, and the front obtained in the median run is shown in the figure. We can see that the fronts obtained by MOEAs are superior to those obtained by RS on C4–C9 with respect to both convergence and diversity. Besides, the Pareto front approximations obtained by NSGA-II are better in convergence for C5, C6, and C8 than those obtained by other algorithms. In contrast to the statistical results, it is hard to see any difference in MOEA performance by only looking at the fronts for test configurations C7 and C9.

To summarize, NSGA-II performs at least as well as DEMO and MOEA/D on C1–C4 and C7, and outperforms both algorithms on C5, C8 and C9. Its efficiency is also comparable to other MOEAs (Table 7). For this reason, we give NSGA-II more attention in the rest of this work.

Figure 3 shows box plots for cumulative hypervolume values obtained before and after parameter tuning on test elevator configurations C7 and C9. The box plots on the left show the results for the ten runs used in the initial phase

Table 6: Adjusted p-values resulting from post hoc analysis with Wilcoxon signed-rank test and Holm's correction.

Pair	Hypervolume	IGD^+
NSGA-II vs. DEMO	0.0117	0.0117
NSGA-II vs. MOEA/D	0.0117	0.0156
DEMO vs. MOEA/D	0.3101	0.2031

Table 7: Average runtime values in seconds for all MOEAs on the test elevator system configurations. All the experiments were run on a 3.50 GHz Intel(R) Xeon(R) E5-2637V4 CPU with 64 GB RAM.

Config.	NSGA-II	DEMO	MOEA/D	RS
C1	17 ± 0	16 ± 1	21 ± 1	5 ± 2
C2	23 ± 1	21 ± 1	46 ± 2	5 ± 2
C3	31 ± 3	28 ± 2	42 ± 5	5 ± 2
C4	325 ± 11	318 ± 5	461 ± 46	34 ± 4
C5	420 ± 11	395 ± 8	672 ± 115	43 ± 14
C6	493 ± 19	432 ± 13	787 ± 113	57 ± 33
C7	1870 ± 62	1998 ± 38	3019 ± 339	115 ± 12
C8	2232 ± 90	2128 ± 38	3249 ± 364	150 ± 29
C9	2562 ± 72	2415 ± 67	3283 ± 812	203 ± 20

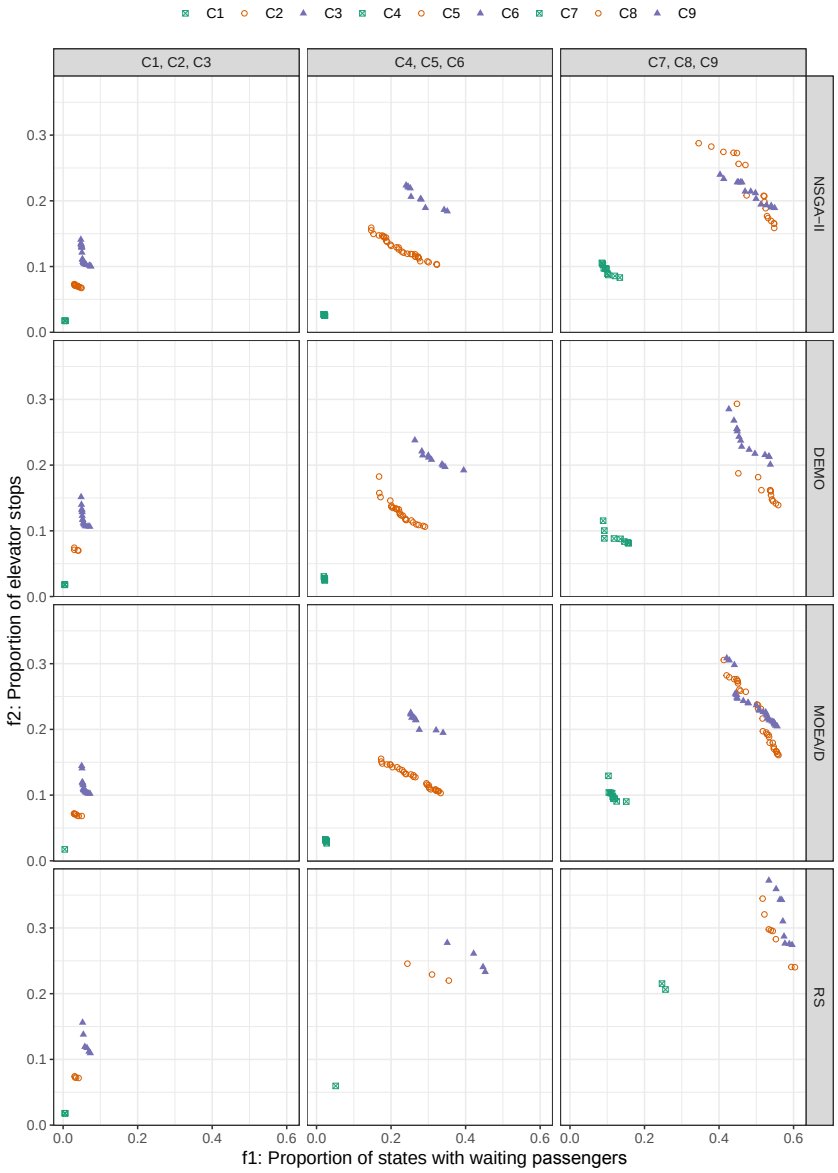

Figure 2: Pareto front approximations for the test elevator system configurations. The first column shows the fronts for test configurations C1–C3, the second column for C4–C6, and the last column for C7–C9. Each row represents one algorithm, from top to the bottom: NSGA-II, DEMO, MOEA/D, and RS.

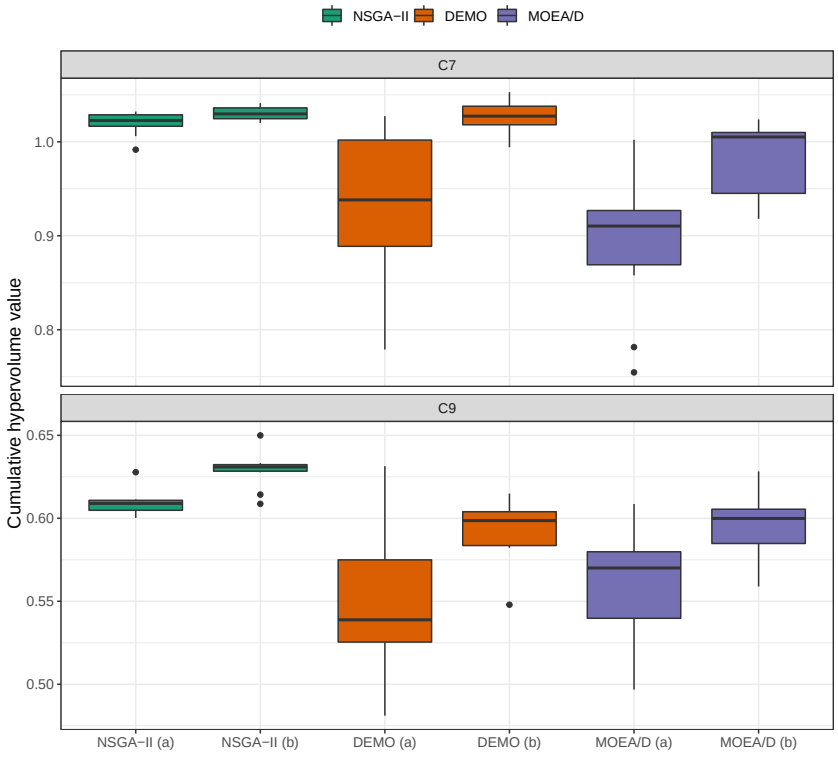

Figure 3: Box plots of cumulative hypervolume values obtained by NSGA-II, DEMO and MOEA/D on test elevator system configurations C7 (top) and C9 (bottom). The cumulative hypervolume values obtained before (a) and after (b) tuning are shown for each algorithm.

of SPOT. These parameters were sampled using the LHS design of experiment method and denote the results before tuning the parameters. The box plots on the right side show the hypervolume values achieved in 31 runs with the tuned parameters from Table 3.

The results show that NSGA-II is less sensitive to parameter selection than DEMO and MOEA/D. While the latter algorithms' performance varies considerably with parameters, NSGA-II is robust over various parameter settings. In particular, the results obtained before tuning NSGA-II are already concentrated around the median hypervolume values. The improvements in the tuning process for NSGA-II are negligible compared to the improvements obtained for DEMO or MOEA/D. For example, on C7, the hypervolume values obtained before tuning NSGA-II are almost as good as those obtained after tuning NSGA-II. Moreover, the results obtained before tuning NSGA-II are already better than the results obtained after tuning MOEA/D. We can also see that DEMO sometimes performs better than NSGA-II but at the expense of performing worse in most runs.

The box plots for C9 show that NSGA-II performs better than DEMO and MOEA/D even with random parameters. Additionally, it is worth noting that NSGA-II using tuned parameters produces three outlier runs: one run achieving much better results and two runs achieving much worse results than the median run. Test elevator configuration C9 is the hardest to solve, and it seems that even the best performing algorithm can sometimes underperform.

In Figure 4, the means of cumulative hypervolume progress are shown for C7 and C9. The x-axis indicates the spent solution evaluations and y-axis the corresponding cumulative hypervolume values. Although NSGA-II and DEMO achieve comparable hypervolume values on C7, NSGA-II is more efficient. NSGA-II needs about 50,000 solution evaluations to converge, while DEMO needs the whole computational budget of 100,000 solution evaluations to obtain the same result. Similar behavior is observed for other test elevator configurations. This further proves that NSGA-II is indeed the best performing algorithm on the test elevator system configurations used in this study.

We also investigated how NSGA-II performs concerning both objectives. In other words, we analyzed the spreads of the obtained Pareto front approximations. We created two constrained single-objective optimization problems, where the first (f_1) and the second (f_2) objective were subject to minimization, separately. Ordered pairs of solutions for

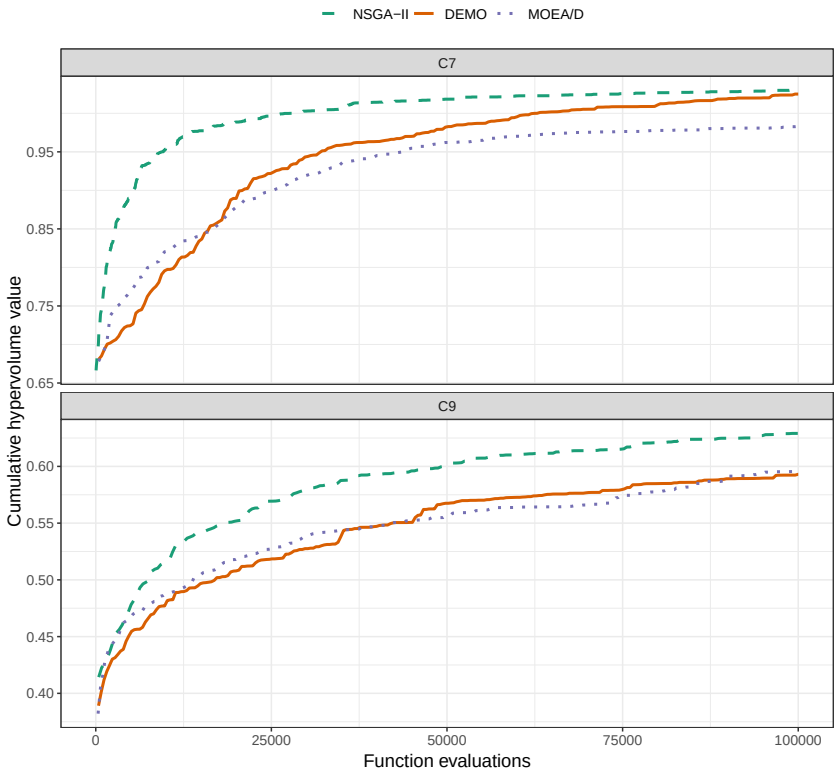

Figure 4: Cumulative hypervolume progress for the test elevator system configurations C7 (top) and C9 (bottom).

both objectives represent approximations of ideal points. To obtain these approximations, the best feasible solutions found in 31 runs of classic differential evolution (DE) [33] were recorded.

The results are shown in Figure 5, where both optimized solutions found by DE and the Pareto front approximations obtained in median runs of NSGA-II are depicted. From the figure, it is evident that it is harder for NSGA-II to find optimal solutions for the second objective, e.g., C7 and C8. This was expected since this objective is strongly negatively correlated with the constraint (Figure 7). On the other hand, we can see that NSGA-II can always find near-optimal solutions concerning the first objective. In conclusion, a typical run of NSGA-II can find a satisfactorily spread Pareto front approximation for each test elevator configuration.

To validate the proposed approach, we also performed an external comparison between NSGA-II and a state-off-the-art method used for solving EGC tion problems. In the related work, multiobjective EGC optimization problems are solved using the weighted-sum approach (WS) [4, 5, 6]. This approach combines the two objectives into a single objective as follows:

$$f^{ws}(\vec{w} \mid \gamma) = \gamma f_1(\vec{w}) + (1-\gamma) f_2(\vec{w}), \tag{8}$$

and transforms the bi-objective EGC optimization problem into a single-objective one:

$$\begin{aligned} \text{minimize} \quad & f^{ws}(\vec{w} \mid \gamma) \\ \text{subject to} \quad & c(\vec{w}) \leq M. \end{aligned} \tag{9}$$

Normally, WS requires a predefined γ that specifies the preference between the objectives. However, we wanted to find a set of trade-off feasible solutions representing approximations for Pareto fronts. For this purpose, we used eleven values for $\gamma \in \{0, 0.1, \ldots, 0.9, 1\}$ specifying various preferences between the objectives and resulting in eleven sub-problems (9) for a given test configuration. For the sake of fair comparison, WS used the same amount of solution evaluations as MOEAs (Table 3). In more detail, the total amount of solution evaluations used for a test configuration was equally divided among eleven sub-problems. For example, 10,000 solution evaluations were used to solve C1–C3 by MOEAs. For this reason, only 909 solutions were allocated to each sub-problem (9). We employed DE with a penalty function approach as a constraint handling technique to solve the resulting optimization sub-problems. Like for MOEAs, the most influential parameters of DE (population size, number of generations, crossover probability and scaling factor) were also tuned using the procedure described in Section 5.2.

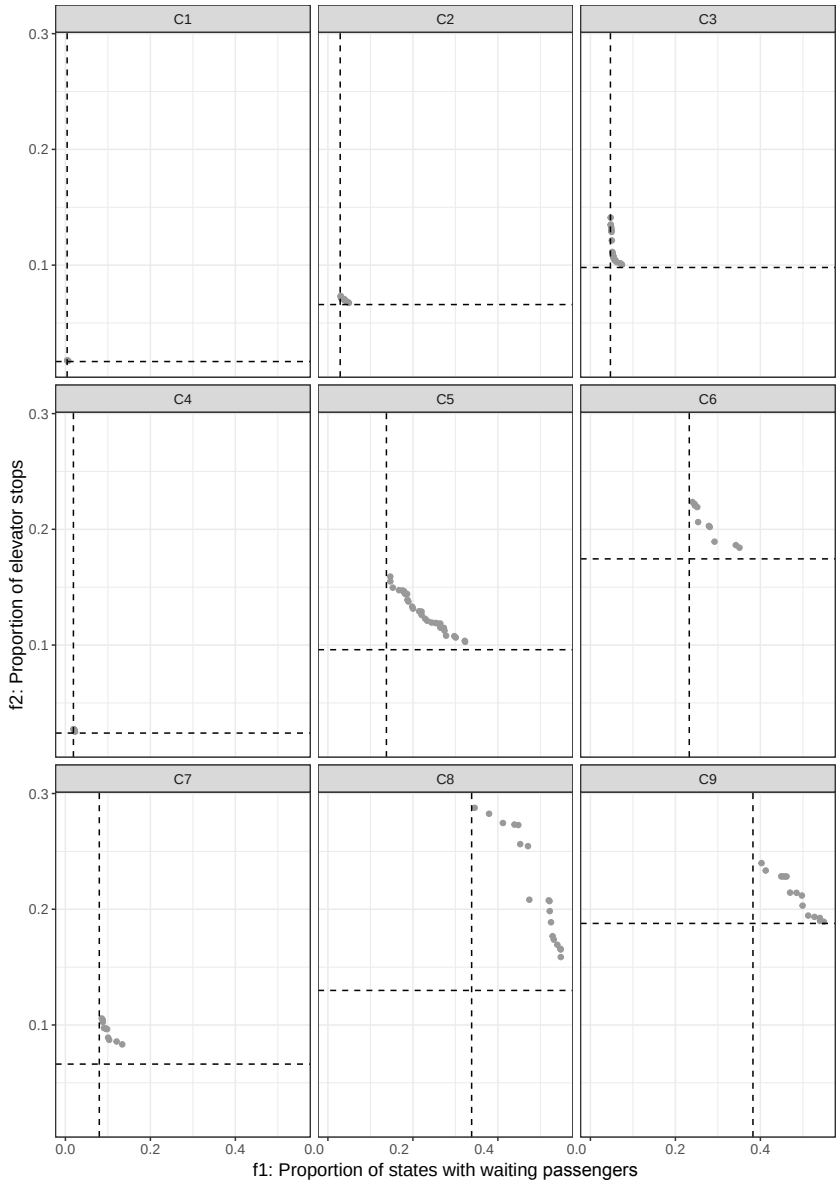

Figure 5: Pareto front approximations resulting from typical runs of NSGA-II. The dashed lines show the minimum objective values found by DE, where each objective was optimized separately. The intersection of the vertical and horizontal lines represents an approximation for the ideal point. The first row shows the results for C1–C3, the second row for C4–C6, and the last row for C7–C9.

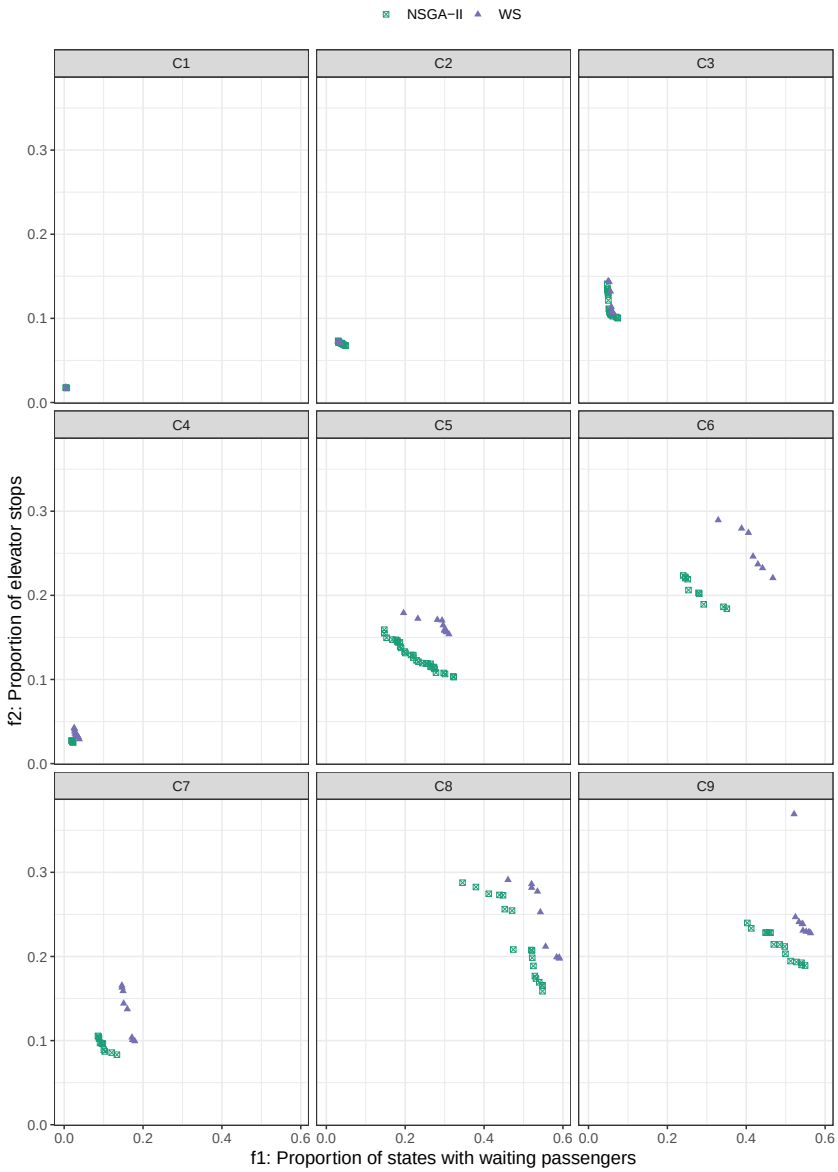

Figure 6: Pareto front approximations resulting from typical runs of NSGA-II and WS. The first row shows the results for C1–C3, the second row for C4–C6, and the last row for C7–C9.

The results are summarized in Figure 6. It shows Pareto front approximations obtained in median runs of NSGA-II and WS. As expected, Pareto front approximations obtained for C1–C3 are comparable. On the other hand, fronts obtained by NSGA-II on C6–C9 dominate those obtained by WS on these problems. Moreover, WS cannot always find 11 nondominated solutions (one per each γ value). These observations confirm the advantage of using true multiobjective optimization over the WS approach. Nevertheless, if the preference between the two objectives is known in advance, one could still use WS instead.

In the rest of this paper, we focus on the specific EGC optimization problem characteristics. We used the results obtained by RS to assess the complexity of the test configurations. As we have already seen, on C1 and C2, hypervolume values obtained by RS are identical to those obtained by MOEAs (Table 4 and Figure 2), indicating that these elevator configurations are trivial to solve. Indeed, C1 and C2 reflect elevator systems operating in small buildings with low passenger traffic. Simple EGC policies, e.g., never skip a passenger, are already suitable solutions quickly found even by RS.

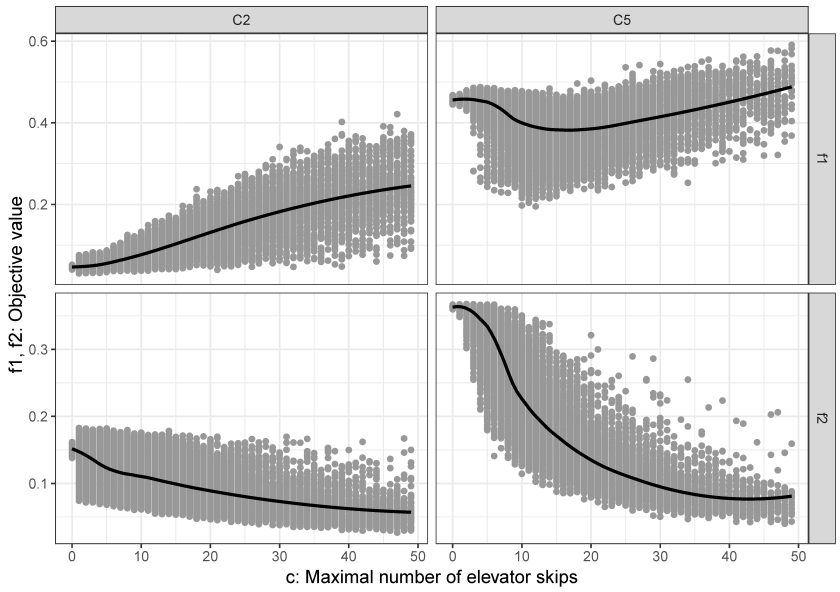

Figure 7: Correlations between the objective and constraint values for the test elevator system configurations C2 (left) and C5 (right).

In contrast, on C3 and C4, the RS algorithm performs worse than MOEAs, obtaining about 2–6% lower hypervolume values (Table 4). The Pareto front approximation for C3 is more sparse than fronts obtained by MOEAs, and the front for C4 is both sparse and not well converged (Figure 2). The same observations are more intensely reflected on C5–C9, where RS obtains about 21–27% worse hypervolume values than MOEAs (Table 4). These results show that test configurations C5–C9 are harder to solve than C1–C4 and provide an insight into why we observe substantial differences in MOEA performance only on C5–C9.

To further investigate the difference between C1–C4 and C5–C9, we analyzed correlations between the objectives and the constraint. Figure 7 shows these correlations for test configurations C2 and C5. For each configuration, 100,000 solutions were randomly sampled. As we can see, the first objective (f_1) is strongly positively correlated (Pearson correlation coefficient $r = 0.89$) with the constraint (c) on C2. The EGC policy that always serves a passenger is a reasonable choice for an elevator system such as C2. The later renders the test configuration C2 easy to solve since optimizing the first objective already improves the constraint violation.

On the other hand, the correlation between the first objective and the constraint is weak (Pearson correlation coefficient $r = -0.31$) on C5. In more detail, we still observe a positive correlation between the objective and the constraint for $10 \leq c \leq 50$, but while this positive correlation persists until $c \leq 4$ on C2, this is not true on C5. This makes this constraint harder to satisfy than the constraint involved in C2.

As expected, the second objective (f_2) is in both cases strongly negatively correlated with the constraint (Pearson correlation coefficient $r = -0.71, -0.89$). The results for other test elevator configurations are not shown here since C1, C3, and C4 behave similar to C2, and C6–C9 behave almost identical as C5.

6 Conclusions

We explored the optimization of EGC, which is a task-relevant in the design and operation of multi-car elevator systems. The problem was formulated as a CMOP involving two conflicting objectives that both have to be minimized, i.e., the proportion of states with waiting passengers and the proportion of elevator stops, and the constraint on the maximum number of elevator skips. The objectives were normalized to compare results over elevator systems with a different number of floors and elevator cars. The S-Ring computational model of an elevator system was used as a prerequisite for numerical optimization. In contrast to most studies in this domain, we exercised the true multiobjective optimization approach that returns approximations of Pareto-optimal solutions to the problem. Three widely used MOEAs, namely NSGA-II, DEMO, and MOEA/D, were deployed for this purpose and tested on nine test elevator system configurations of various complexity.

The experimental evaluation included tuning the algorithm parameters, systematic experiments on the test elevator configurations, and statistical analysis of the results. As expected, the more complex the elevator configuration, the more evident becomes the superiority of MOEAs over the baseline approach, i.e., random search. While the computational efficiency of the three tested algorithms is comparable as it mainly depends on the cost of the S-Ring simulation, in terms of the effectiveness, NSGA-II performs best on average, and its parameter setting was found the most robust in the tuning process.

From the application point of view, the methodology represents a valuable tool, and the results offer new insights into the problem domain to decision-makers involved in the elevator system configuring and EGC design. The identified sets of nondominated solutions allow for trading between the objective values and the analysis of correlations between the objectives and the constraint for a better understanding of the problem.

The key directions of our further work in this domain include analyzing the produced trade-off control policies in the design space and enhancing the methodology for applications in advanced real-world elevator systems. Of particular interest in the latter case will be dynamically changing operating conditions of the elevator systems where, unlike in the current study, the systems performance will be optimized over different traffic situations.

Acknowledgments

This work is part of a project that has received funding from the *European Union's Horizon 2020 research and innovation program* under Grant Agreement no. 692286. We acknowledge financial support from the Slovenian Research Agency (young researcher program and research core funding no. P2-0209). The work is also part of the Slovenian-German research collaboration supported by the Slovenian Research Agency (project BI-DE/20-21-019) and the German Academic Exchange Service (project 57515062). T. Bartz-Beielstein acknowledges support from the *Ministerium für Kultur und Wissenschaft des Landes Nordrhein-Westfalen* in the funding program *FH Zeit für Forschung* under the grant number 005-1703-0011 (project OWOS) and support from the *German Federal Ministry of Education and Research* in the funding program *Forschung an Fachhochschulen* under the grant number 13FH007IB6 (project KOARCH).

References

[1] T. Bartz-Beielstein, M. Preuss, S. Markon, Validation and optimization of an elevator simulation model with modern search heuristics, in: T. Ibaraki, K. Nonobe, M. Yagiura (Eds.), Metaheuristics: Progress as Real Problem Solvers, Springer, Berlin, Heidelberg, New York, 2005, pp. 109–128. doi:10.1007/0-387-25383-1_5.

[2] A. Vodopija, J. Stork, T. Bartz-Beielstein, B. Filipič, Model-based multiobjective optimization of elevator group control, in: B. Filipič, T. Bartz-Beielstein (Eds.), International Conference on High-Performance Optimization in Industry, HPOI 2018 : Proceedings of the 21st International Multiconference Information Society, IS 2018, Jožef Stefan Institute, Ljubljana, Slovenia, 2018, pp. 43–46.

[3] S. Markon, A solvable simplified model for elevator group control studies, in: 2015 IEEE 4th Global Conference on Consumer Electronics, GCCE, IEEE, 2015, pp. 56–60. doi:10.1109/GCCE.2015.7398739.

[4] H. M. Hakonen, A. Rong, R. Lahdelma, Multiobjective optimization in elevator group control, in: P. Neittaanmäki, T. Rossi, S. Korotov, E. Oñate, J. Périaux, D. Knörzer (Eds.), European Congress on Computational Methods in Applied Sciences and Engineering, ECCOMAS 2004, 2004, 17 pages.

[5] Y. G. Sahin, S. Uzunbayir, B. Akcay, E. Yildiz, Real-time monitoring of elevators to reduce redundant stops and energy wastage, in: Proceedings of the 2013 International Conference on Systems, Control and Informatics, 2013, pp. 264–269.

[6] T. Tyni, J. Ylinen, Evolutionary bi-objective optimisation in the elevator car routing problem, European Journal of Operational Research 169 (2006) 960–977. doi:10.1016/j.ejor.2004.08.027.

[7] T. Mahmud, S. M. Saiduzzaman, S. S. Ahbab, S. S. Saud Nikor, A simplified, novel and efficient approach to operate a group of elevators using a common control, in: 2019 IEEE International Conference on Robotics, Automation, Artificial-intelligence and Internet-of-Things, RAAICON, IEEE, 2019, pp. 131–134. doi:10.1109/RAAICON48939.2019.56.

[8] P. E. Utgoff, M. E. Connell, Real-time combinatorial optimization for elevator group dispatching, IEEE Transactions on Systems, Man, and Cybernetics - Part A: Systems and Humans 42 (1) (2012) 130–146. doi:10.1109/TSMCA.2011.2157134.

[9] A. Fujino, T. Tobita, K. Segawa, K. Yoneda, A. Togawa, An elevator group control system with floor-attribute control method and system optimization using genetic algorithms, IEEE Transactions on Industrial Electronics 44 (4) (1997) 546–552. doi:10.1109/41.605632.

[10] D. L. Pepyne, C. G. Cassandras, Optimal dispatching control for elevator systems during uppeak traffic, IEEE Transactions on Control Systems Technology 5 (6) (1997) 629–643. doi:10.1109/87.641406.

[11] J.-M. Kuusinen, M. Ruokokoski, J. Sorsa, M.-L. Siikonen, Linear programming formulation of the elevator trip origin-destination matrix estimation problem, in: B. Vitoriano, F. Valente (Eds.), Proceedings of the 2nd International Conference on Operations Research and Enterprise Systems, ICORES 13, 2013, pp. 298–303. doi:10.5220/0004338502980303.

[12] T. Miyamoto, S. Yamaguchi, MceSim: A multi-car elevator simulator, IEICE Transactions Fundamentals E91 (11) (2008) 3207–3214. doi:10.1093/ietfec/e91-a.11.3207.

[13] S. Markon, D. V. Arnold, T. Bäck, T. Beielstein, H.-G. Beyer, Thresholding—A selection operator for noisy ES, in: Proceedings 2001 Congress on Evolutionary Computation, CEC, IEEE, Piscataway NJ, 2001, pp. 465–472. doi:10.1109/CEC.2001.934428.

[14] T. Bartz-Beielstein, K. E. Parsopoulos, M. N. Vrahatis, Design and analysis of optimization algorithms using computational statistics, Applied Numerical Analysis & Computational Mathematics 1 (2) (2004) 413–433. doi:doi.org/10.1002/anac.200410007.

[15] R. A. Howard, Dynamic Programming and Markov Processes, MIT Press, Cambridge, 1960.

[16] A. Onat, S. Markon, H. Kita, Y. Nishikawa, A Benchmark Problem for Evaluating Reinforcement Learning Methods, Tech. rep. (2002).

[17] M. Ruokokoski, J. Sorsa, M.-L. Siikonen, H. Ehtamo, Assignment formulation for the elevator dispatching problem with destination control and its performance analysis, European Journal of Operational Research 252 (2) (2016) 397–406. doi:https://doi.org/10.1016/j.ejor.2016.01.019.

[18] N. Takahashi, S. Markon, A. Onat, Multi-objective optimization of the design of an elevator linear motor, in: 2013 IEEE Power Energy Society General Meeting, IEEE, 2013, pp. 1–5. doi:10.1109/PESMG.2013.6672412.

[19] T. Ishii, Elevators for skyscrapers, IEEE Spectrum 31 (9) (1994) 42–46. doi:10.1109/6.309960.

[20] S. Markon, Y. Komatsu, A. Yamanaka, A. Onat, E. Kazan, Linear motor coils as brake actuators for multi-car elevators, in: 2007 International Conference on Electrical Machines and Systems, ICEMS, IEEE, 2007, pp. 1492–1495.

[21] Y. Okamoto, N. Takahashi, Minimization of driving force ripple of linear motor for rope-less elevator using topology optimization technique, Journal of Materials Processing Technology 181 (1) (2007) 131–135. doi:10.1016/j.jmatprotec.2006.03.057.

[22] A. Onat, E. Kazan, N. Takahashi, D. Miyagi, Y. Komatsu, S. Markon, Design and implementation of a linear motor for multicar elevators, IEEE/ASME Transactions on Mechatronics 15 (5) (2010) 685–693. doi:10.1109/TMECH.2009.2031815.

[23] C. Gurbuz, E. Kazan, A. Onat, S. Markon, Linear motor for multi-car elevators, design and position measurement, Turkish Journal of Electrical Engineering & Computer Sciences 19 (6) (2011) 827–838. doi:10.3906/elk-1007-594.

[24] S. Markon, H. Kita, H. Kise, T. Bartz-Beielstein (Eds.), Control of Traffic Systems in Buildings, Springer, Berlin, Heidelberg, New York, 2006.

[25] K. Deb, A. Pratap, S. Agarwal, T. Meyarivan, A fast and elitist multiobjective genetic algorithm: NSGA-II, IEEE Transactions on Evolutionary Computation 6 (2) (2002) 182–197. doi:10.1109/4235.996017.

[26] T. Robič, B. Filipič, DEMO: Differential evolution for multiobjective optimization, in: C. A. Coello Coello, A. Hernández Aguirre, E. Zitzler (Eds.), Proceedings of the Third International Conference on Evolutionary Multi-Criterion Optimization, EMO 2005, Vol. 3410 of Lecture Notes in Computer Science, Springer, Berlin, Heidelberg, 2005, pp. 520–533. doi:10.1007/978-3-540-31880-4_36.

[27] Q. Zhang, H. Li, MOEA/D: A multiobjective evolutionary algorithm based on decomposition, IEEE Transactions on Evolutionary Computation 11 (6) (2007) 712–731. doi:10.1109/TEVC.2007.892759.

[28] F. Campelo, L. S. Batista, C. Aranha, The MOEADr package: A component-based framework for multiobjective evolutionary algorithms based on decomposition, Journal of Statistical Software 92 (6) (2020) 1–39. doi:10.18637/jss.v092.i06.

[29] T. Bartz-Beielstein, C. W. Lasarczyk, M. Preuss, Sequential parameter optimization, in: 2005 IEEE Congress on Evolutionary Computation, CEC, IEEE, 2005, pp. 773–780. doi:10.1109/CEC.2005.1554761.

[30] R Core Team, R: A Language and Environment for Statistical Computing, R Foundation for Statistical Computing, Vienna, Austria (2013).
URL http://www.R-project.org/

[31] A. Vodopija, egccmop: Elevator group control as a constrained multiobjective optimization problem (2020).
URL https://github.com/vodopijaaljosa/egccmop

[32] GNU General Public License, version 3.
URL http://www.gnu.org/licenses/gpl.html

[33] K. V. Price, R. M. Storn, J. A. Lampinen, Differential Evolution, Natural Computing Series, Springer, Berlin, Heidelberg, 2005. doi:10.1007/3-540-31306-0.